

Green full polymer flexible transparent electrodes showing versatile switching behaviors based on either counterion transport or nanoarea crystallization

Jingwen Liao, Mingjin Yang, Wenfeng Liu, Yahong Zhou, Xiaofeng Bi, and Hai Yuan

Electronic Supplementary Material

Abbreviations

AFM: atomic force microscopy

CFU: colony forming unit

EDOT: 3,4-ethylenedioxythiophene

DMMAPS: 3-(N,N-dimethylmyristylammonio)propanesulfonate

DPEHA: dipentaerythritol hexaacrylate

EHA: 2-ethylhexyl acrylate

FOEMA: 2-(perfluorooctyl)ethyl methacrylate

FPDTPy: 1-(perfluorophenyl)-2,5-di(thiophen-2-yl)-1H-pyrrole

FPFTEs: full polymer flexible transparent electrodes

FTIR: fourier transform infrared

GPC: gel permeation chromatography

¹H-NMR: hydrogen nuclear magnetic resonance

HRTEM: high-resolution transmission electron microscopy

ITO: indium tin oxides

LB: lysogeny broth

PBS: phosphate buffered solution

PET: poly(ethylene terephthalate)

PTSA: p-toluene sulphonic acid

THF: tetrahydrofuran

TMPTA: trimethylolpropane triacrylate

SCA: static contact angle

SEM: scanning electron microscopy

STEM: scanning transmission electron microscopy

UV: ultraviolet

UV–Vis–NIR: ultraviolet–visible–near infrared

XPS: X-ray photoelectron spectroscopy

XRD: X-ray diffraction

Experimental (partly)

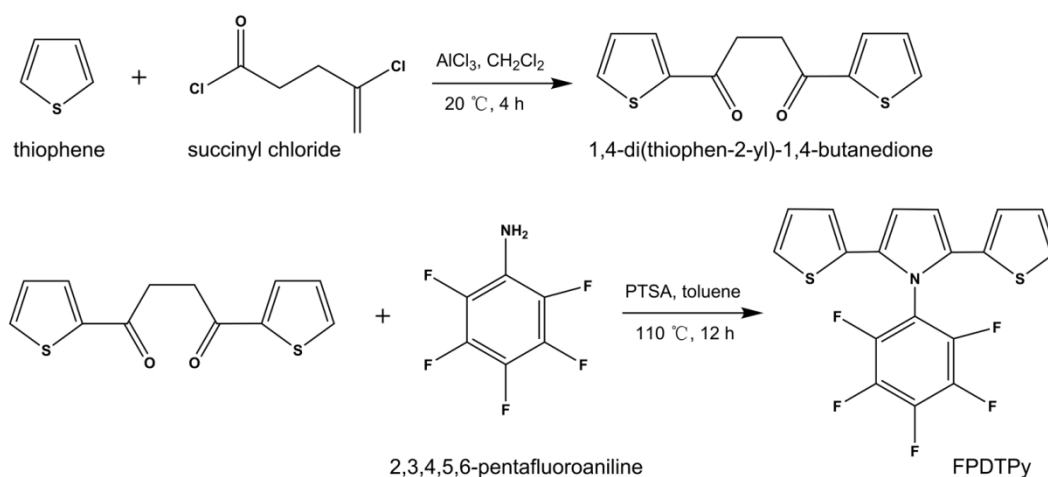
Chemicals

If not otherwise specified, the chemicals of analytical grade were purchased from Aladdin Chem Co., and used without further treatment. TMPTA and EHA with 98% of purity were acquired from Macklin CO., DPEHA and FOEMA with 99% of purity were supplied by Rhawn Chem CO., $\text{Ph}_2\text{I}^+\text{PF}_6^-$ with $\geq 98\%$ of purity was obtained from Sigma–Aldrich Co, Darocur 4265 was provided by Kunshan Century Dragon Chemical Co.

Synthesis of FPDTPy

According to Toppare's report,¹ first, 1,4-di(thiophen-2-yl)-1,4-butanedione was synthesized. Typically, a solution of thiophene (0.12 mol) and succinyl chloride (0.05 mol) in CH_2Cl_2 (6 ml) was added drop by drop into a CH_2Cl_2 suspension (15 mL) containing alchlor (AlCl_3 , 0.12 mol), and followed by stirring at 20 °C for 4 h. Then, an ice concentrated hydrochloric acid solution (5 mL) was poured into the mixture. The obtained green organic solution was washed with concentrated sodium bicarbonate several times. After drying under vacuum, 1,4-di(thiophen-2-yl)-1,4-butanedione was produced and kept in ethanol prior to use. Further, 1,4-di(thiophen-2-yl)-1,4-butanedione (5 mmol), 2,3,4,5,6-pentafluoroaniline (7 mmol), p-toluene sulphonic acid (PTSA, 0.58 mmol) and toluene (20 mL) were mixed in a round-bottomed flask using magnetic stirring under the protection of nitrogen. The mixture was refluxed at 110 °C for 12 h in nitrogen atmosphere. By the removal of toluene and SiO_2 flash column chromatography (elution with dichloromethane), a light brown compound, that was, FPDTPy, was synthesized.

The synthetic route of FPDTPy was displayed in Scheme S1:



Scheme S1 The synthesis route of the FPDTPy.

Characterization of materials

XRD spectroscopy (BrukerD8 Advanced, Germany) was used to record the crystalline states of specimens. XPS (Kratos Axis Ultra DLD, Britain), FTIR spectrometer (Bruker Vector 33, Germany) and Raman spectrometer (HJY LabRAM Aramis, France) were applied to analyze the chemical composition of specimens. $^1\text{H-NMR}$ spectrometer (Magritek GmbH Spinsolve 60, Germany) was utilized to qualitatively characterize FPDTPy using CDCl_3 as the solvent. The molecular weights of the resultants were determined by GPC (WATERS 1515, Germany) using THF as the eluent and polystyrenes as the standards at room temperature. AFM (Bruker Dimension Icon, USA) was employed to collect phase images of specimens in the tapping mode. The electrochemical activity of specimens was tested by cyclic voltammetry carried out in the three-electrode system. The studies on the optoelectrochemical and kinetic behaviors were conducted using a UV-Vis-NIR spectrophotometer under the control of the electrochemical station (CH Instrument, CHI 660E, China). The water SCA measurements of specimens were performed using a surface contact angle analyzer (KSV Helsinki CAM200, Finland) with a $1\ \mu\text{L}$ water droplet at ambient temperature. The electrical conductivity and haze factor of FPFTEs were recorded by a four-probe meter (4 Probes Tech RTS-4, China) and transmittance/haze meter (ShenGuang WGT-S, China), respectively. SEM (Hitachi S-4800, Japan) and HRTEM (JEOL JEM-2100F, Japan) were employed to examine the surface topography and phase composition of specimens, respectively. STEM imaging and line-profile analysis were carried out using HRTEM (JEOL JEM-2100F, Japan), and the STEM specimens were prepared by a focused ion beam (FIB, FEI Helios600i, USA) with the *in situ* lift-out technique. Using a universal testing machine (Oberthur UTM5504, China), the mechanical assays were conducted to determine the flexural and tensile properties as per ASTM D790 and D638, at a speed of 10 and $5\ \text{mm min}^{-1}$, respectively.

Bacterial adhesion on FPFTEs

Gram-negative *Escherichia coli* (ATCC 25922) were chosen as a bacteria model to assess the antibacterial ability of specimens. The bacteria were cultured in lysogeny

broth (LB) medium (1% w/v tryptone, 0.3% w/v yeast extract, and 0.5% w/v NaCl). The bacterial pellet obtained from ATCC was rehydrated in 0.5 mL of LB, and several drops of the suspension were immediately placed and streaked on an agar slant of LB. The agar-plate was then incubated aerobically at 37 °C for 24 h. Overnight cultures of *Escherichia coli* were made by aseptically transferring a single colony forming unit (CFU) into 10 mL of LB, followed by aerobic incubation under shaking at 200 rpm (37 °C) for 16 h. The bacteria from the overnight cultures were used to inoculate fresh media to a final concentration of 10^5 CFU/mL. Bacteria were then incubated in the same manner as the overnight cultures, until they reached the mid log phase as determined by optical density measurement at 600 nm. Then, the cultures were centrifuged at 4000 rpm for 5 min (Sorvall RC 5B Plus Centrifuge) followed by removal of the supernatant. The bacterial pellet was resuspended in 500 μ L of LB. This suspension was then transferred to a 2 mL centrifuge tube and centrifuged at 5500 rpm for 3 min (Fischer Scientific AccuSpin Micro Centrifuge). The supernatant was carefully removed, and the bacterial pellet was resuspended in sterile PBS to a final concentration of 10^6 CFU/mL. Then, 1 mL of suspension was added to each well containing a specimen and incubated under shaking at 200 rpm (37 °C). After 2 h incubation, the bacterial suspension was removed, and then the surfaces were washed twice with 1 mL of PBS by pipetting. At the end of the experiment, adherent bacteria on specimens were fixed with 500 μ L of 2% glutaldehyde for 30 min, followed by dehydration in a series of increasing alcohol baths (50% ethanol for 10 min, 70% ethanol for 10 min, 90% ethanol for 10 min, followed by a 1 mL wash with 100% ethanol). For visualization of bacterial adhesion on specimen, 500 μ L of 5 μ M SYTO9 Green Fluorescent Nucleic acid stain (Invitrogen, S3485) was added to each well containing a specimens, protected from light, and incubated for 20 min. Specimens were then washed 3 times with 1 mL of PBS by pipetting the PBS up-and-down twice. Finally, the specimens were secured onto a clean microscope slide and viewed under a Fluorescent Microscope (Nikon Eclipse TE2000-U, Japan).

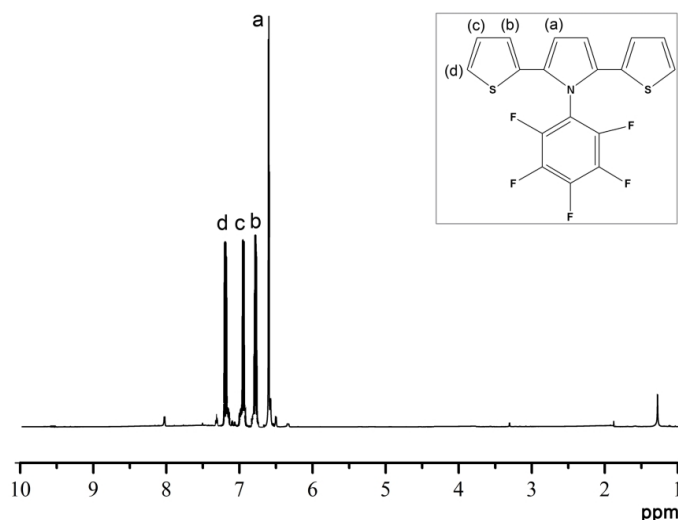


Fig. S1 $^1\text{H-NMR}$ spectrum of FPDTPy. δ_{H} (CDCl_3): 6.65 (s, 2H, pyrrolyl), 6.83 (d, 2H, $J = 3.41$ Hz, 3-thienyl), 6.95 (dd, 2H, $J = 4.69$ Hz, 3.41 Hz, 4-thienyl), 7.20 (d, 2H, $J = 4.69$ Hz, 5-thienyl).

Table S1 The solvent-free intermiscible stability of ink prepared by the various mass ratios of conducting phase precursor to flexible phase precursor and various amounts of compatibility additive (DMMAPS) and two types of photoinitiators ($\text{Ph}_2\text{I}^+\text{PF}_6^-$ and Darocur 4265). When the ink was homogeneous, indicating an intermiscible state of current system. While the ink was heterogeneous (*i.e.*, stratification between two or several phases), implying an immiscible state. Herein, if the immiscible state appeared after 0, 3 and 15 days, and the ink was labelled “ \times ”, “ \checkmark ”, and “ $\checkmark \checkmark$ ”, respectively.

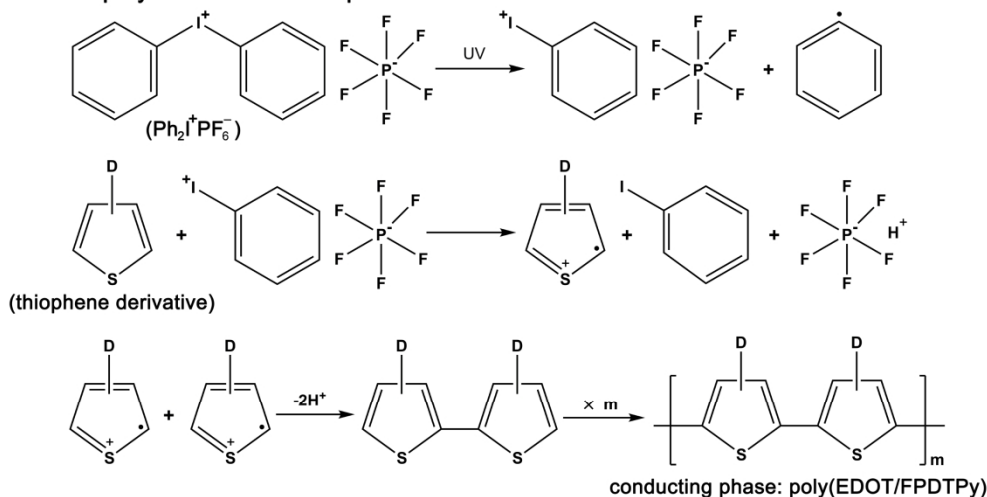
It was decided that, under the 7 : 3 of mass ratio of conducting phase precursor to flexible phase precursor, the amount of $\text{Ph}_2\text{I}^+\text{PF}_6^-$ relative to mass of conducting phase precursor was 7%, the amount of Darocur 4265 relative to mass of flexible phase precursor was 3%, and the amount of EMMAPS relative to total mass of conducting phase precursor and flexible phase precursor was 6%.

^{#1} For conducting phase precursor, the molar ratio of EDOT to FPDTPy was 3 : 2, and for flexible phase precursor, the molar ratio of FOEMA (*F1*), EHA (*F1*), TMPTA (*F3*) to DPEHA (*F6*) was 3 : 3 : 8 : 6. ^{#2} Without both $\text{Ph}_2\text{I}^+\text{PF}_6^-$ and Darocur 4265. ^{#3} With 6% DMMAPS but without Darocur 4265. ^{#4} With 6% DMMAPS but without $\text{Ph}_2\text{I}^+\text{PF}_6^-$.

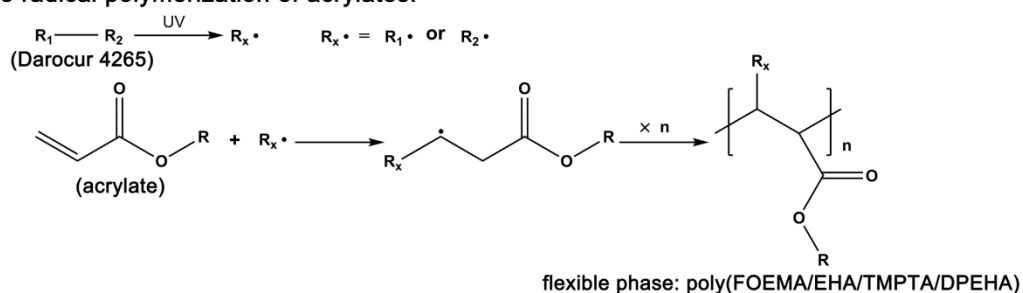
conducting phase precursor : flexible phase precursor #1	9.0 : 1.0	8.5 : 1.5	8.0 : 2.0	7.5 : 2.5	7.0 : 3.0	6.5 : 3.5	6.0 : 4.0
---	-----------	-----------	-----------	-----------	-----------	-----------	-----------

DMMAPS #2	1%	×	×	×	×	×	×	×
	2%	×	×	×	×	×	✓	✓
	4%	×	✓	✓	✓	✓	✓	✓ ✓
	6%	✓	✓	✓	✓	✓ ✓	✓ ✓	✓ ✓
	8%	✓ ✓	✓ ✓	✓ ✓	✓ ✓	✓ ✓	✓ ✓	✓ ✓
Ph ₂ I ⁺ PF ₆ ⁻ #3	1%	✓ ✓	✓ ✓	✓ ✓	✓ ✓	✓ ✓	✓ ✓	✓
	4%	✓ ✓	✓ ✓	✓ ✓	✓ ✓	✓ ✓	✓ ✓	✓
	7%	✓ ✓	✓ ✓	✓ ✓	✓ ✓	✓ ✓	✓	✓
	10%	✓	✓	✓	✓	✓	×	×
Darocur 4265 #4	1%	✓	✓	✓	✓ ✓	✓ ✓	✓ ✓	✓ ✓
	3%	×	✓	✓	✓	✓ ✓	✓ ✓	✓ ✓
	5%	×	×	✓	✓	✓	✓	✓ ✓
	7%	×	×	×	×	×	×	✓

cationic polymerization of thiophene derivatives:



free radical polymerization of acrylates:



Scheme S2 The mechanism of UV-initiated cationic polymerization of thiophene derivatives and free radical polymerization of acrylates.

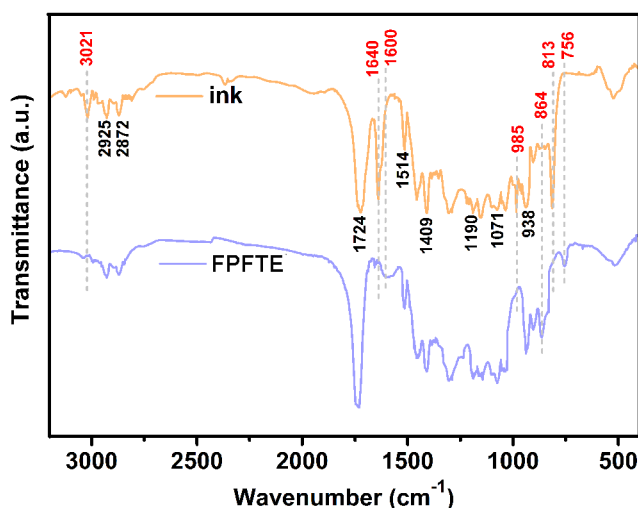


Fig. S2 FTIR spectra of UV-printed ink (orange) and FPFTE (blue). In the spectrum of ink, a series of characteristic peaks appeared at 3021 cm⁻¹ (C-H_α stretching vibration of thiophene ring in EDOT and FPDTPy), 2925 and 2872 cm⁻¹ (C-H stretching vibrations of the oxyethylene ring in EDOT), 1724 cm⁻¹ (C=O stretching vibration in four polyacrylate monomers), 1640 cm⁻¹ (C=C stretching vibration in four polyacrylate monomers), 1514 cm⁻¹ (C-F stretching vibration in FPDTPy and

FOEMA), 1409 cm^{-1} (aromatic C=C vibration in FPDTPy), 1190 cm^{-1} (C-O-C stretching vibration in EDOT and four polyacrylate monomers), 1071 cm^{-1} (aromatic C=C-F vibration in FPDTPy), 985 cm^{-1} (=C-H₂ out of plane twist vibration in four polyacrylate monomers), 938 cm^{-1} (=C-S stretching vibration of thiophene ring in EDOT and FPDTPy), 813 cm^{-1} (=C-H₂ deformation vibration in four polyacrylate monomers). By contrast, in the spectrum of FPFTE, the peak at 3021 cm^{-1} completely disappeared, due to the polymerization of 2,5-positions of thiophene ring in EDOT and FPDTPy. Similarly, the three peaks at 1640, 985 and 813 cm^{-1} were not visible any more, resulting from the break of C=C of acrylate groups. Whereas, two new peaks presented at 864 and 756 cm^{-1} , derived from the C-H_β out-plane bending vibration of 2,5-disubstituted thiophene ring and C-S stretching vibration, respectively. Moreover, a fresh broad peak appeared at around 1600 cm^{-1} , which was an evidence of the presence of polyconjugation. In brief, under exposure of UV-radiation, both the cationic polymerization of conducting phase precursor (EDOT and FPDTPy) and the free radical polymerization of flexible phase precursor (four polyacrylate monomers) were initiated with the assistance of composite photoinitiator. That was, the FPFTEs were produced by UV-printing.

Table S2 Molecular weights of the polymers recognized by GPC. *M_n*: number-average molecular weight, *M_w*: weight-average molecular weight, PDI: polydispersity indices (*M_w*/*M_n*). Because the conducting phase (poly(EDOT/FPDTPy)) and flexible phase (poly(FOEMA/EHA/TMPTA/DPEHA)) were “mixed” to form FPFTEs in a physical manner, the two phases had its own molecular weight, that was, *M_n*: 13.8 KDa for conducting phase and 30.6 KDa for flexible phase, *M_w*: 21.0 KDa for conducting phase and 44.9 KDa for flexible phase. Noteworthy, the pure poly(EDOT/FPDTPy) (*i.e.*, EDOT and FPDTPy were copolymerized without the four type of acrylates) and the pure poly(FOEMA/EHA/TMPTA/DPEHA) (*i.e.*, the four type of acrylates were copolymerized without both EDOT and FPDTPy) show a higher both *M_w* and *M_n* than conducting phase and flexible phase, respectively. This possibly implied that during the simultaneous proceeding of cationic polymerization and free radical polymerization, the polymeric chain formation of one phase have certain inhibiting effect on the longer polymeric chain formation of another phase mutually.

polymer	<i>M_n</i> (KDa)	<i>M_w</i> (KDa)	PDI
pure poly(EDOT/FPDTPy)	18.2	25.3	1.39
pure poly(FOEMA/EHA/TMPTA/DPEHA)	33.7	51.2	1.52
poly(EDOT/FPDTPy) in FPFTEs	13.8	21.0	1.52
poly(FOEMA/EHA/TMPTA/DPEHA) in FPFTEs	30.6	44.9	1.47

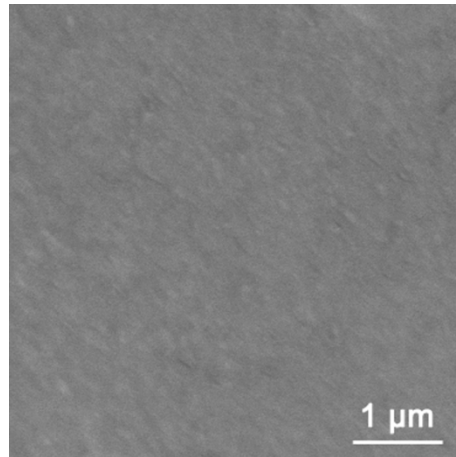


Fig. S3 SEM image of FPFTEs. The SEM image indicated a very smooth surface of FPFTEs.

Table S3 The effect of thickness of FPFTEs on sheet resistance and optical transmittance. As the thickness was increased, the sheet resistance of the FPFTEs gradually decreased and the optical transmittance declined step by step.

thickness (mm)	sheet resistance ($\Omega \text{ sq}^{-1}$)	optical transmittance (%)
0.2	248.4 \pm 19.2	91.7 \pm 1.2
0.3	160.4 \pm 20.0	87.1 \pm 1.5
0.4	117.9 \pm 9.5	83.3 \pm 0.9
0.6	81.9 \pm 6.8	79.0 \pm 0.5

Table S4 The cost, environmental friendliness, scale of production and adhesion to substrates of silver nanowire-based FTEs, grapheme/graphene oxide-based FTEs and carbon nanotube-based FTEs and FPFTEs. The cost, environmental friendliness, scale of production and adhesion to substrates of the first three types of FTEs (silver nanowire-based FTEs, grapheme/graphene oxide-based FTEs and carbon nanotube-based FTEs) in Table S4 were collected and analyzed by some published references,²⁻⁶ market survey reports,⁷⁻⁹ and quotations from suppliers.

^{#1} The four types of FTEs had less than 150 $\Omega \text{ sq}^{-1}$ of sheet resistance and more than 80% of optical transmittance. ^{#2} The overall cost: the material cost, but not the product price. ^{#3} The environmental friendliness: whether and the amount of organic/corrosive/toxic solvents or reagents were used. ^{#4} The scale of production: for large-scale production, whether the expensive precision equipments were needed and how the stability of electrical and optical properties was.

type of FTE #1	cost (dollars/m ²) #2	environmental friendliness #3	scalable production #4	adhesion to substrates
silver nanowire-based FTEs	10~20	moderate	moderate	poor
grapheme/graphene oxide-based FTEs	> 20	poor	moderate	poor
carbon nanotube-based FTEs	> 20	poor	no	poor
FPFTEs	≈ 2	good	yes	good

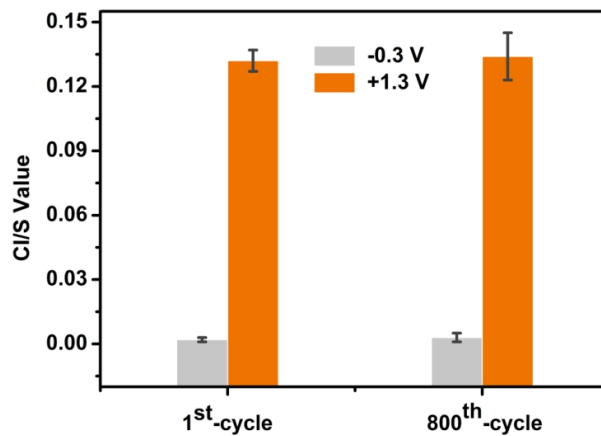


Fig. S4 The change into C/I/S values of FPFTEs after undergoing 800 cycles of switching. After undergoing 800 cycles of switching, the C/I/S values of FPFTEs in both switch (-0.3) and switch (+1.3) remained almost the same as the first cycle of switching.

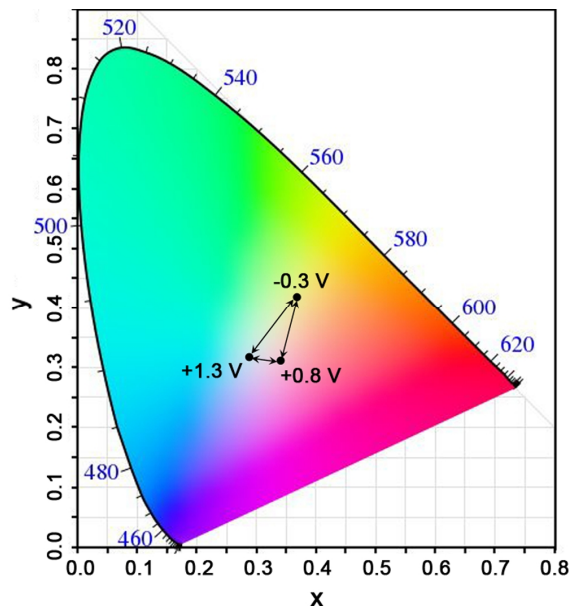


Fig. S5 CIE color coordinates of FPFTEs in response to various electrical stimuli. Through the response to various electrical stimuli, the FPFTEs reversibly became

yellow at -0.3 V, pink at +0.8 V, and cyan at +1.3 V. In CIE color coordinates, the FPFTEs were at (0.364, 0.420) for yellow, (0.341, 0.310) for pink and (0.284, 0.319) for cyan.

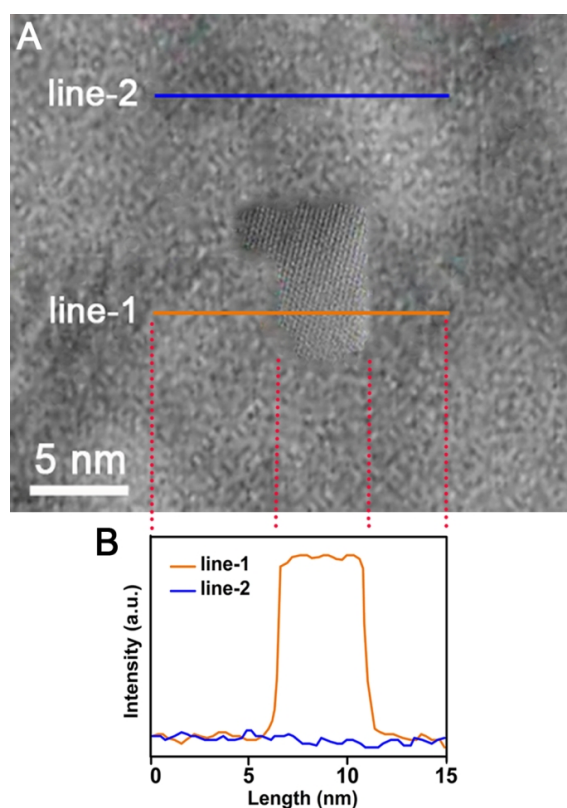


Fig. S6 (A) STEM image of FPFTEs after response to an electrical stimulus of +2.0 V. (B) STEM-EDS records of line-profile analysis for S element along the selected line-1 (containing both amorphous area and crystalline nanoarea) and line-2 (containing only amorphous area alone) in (A). Clearly, The crystalline nanoarea showed a much higher intensity of S element than amorphous area, indicating a likely fact that crystalline nanoareas were exclusively composed of poly(EDOT/FPDTPy).

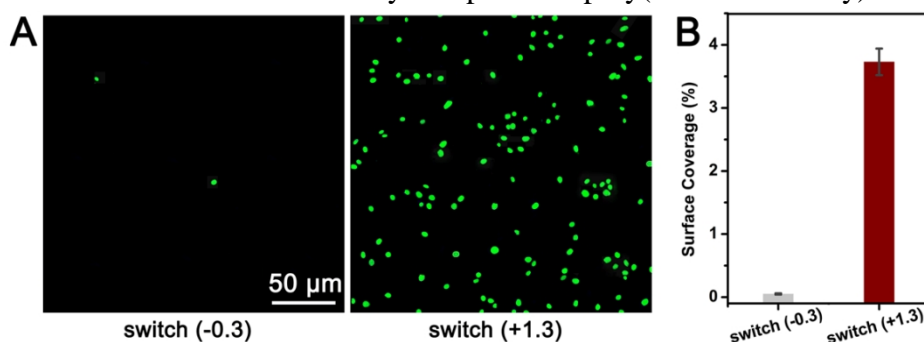


Fig. S7 (A) Fluorescence images of SYTO9 stained *Escherichia coli* adhering on FPFTEs in switch (-0.3) and switch (+1.3) for 2h. (B) The plot of surface coverage of bacteria calculated from (A). As a bacteria model, *Escherichia coli* was chosen to assess antibacterial ability. There were much fewer adherent *Escherichia coli* on the surfaces of FPFTEs in switch (-0.3) than that in switch (+1.3), resulting possibly from

switching behavior of wettability. In more detail, the surfaces of FPFTEs in switch (-0.3) were highly hydrophobic and thus went against the adhesion of bacteria by restraining the early adhesion of protein or glycoprotein. In comparison, the FPFTEs in switch (+1.3) having an appropriately hydrophilic surface (about 80°) were conducive to the firm adhesion of bacteria.

Reference:

1. E. Sahin, E. Sahmetlioglu, I. M. Akhmedov, C. Tanyeli and L. Toppare, *Org. Electron.*, 2006, **7**, 351-362.
2. J. Kwon, Y. D. Suh, J. Lee, P. Lee, S. Han, S. Hong, J. Yeo, H. Lee and S. H. Ko, *J. Mater. Chem. C*, 2018, **6**, 7445-7461.
3. Q. Zheng, Z. Li, J. Yang and J.-K. Kim, *Prog. Mater. Sci.*, 2014, **64**, 200-247.
4. C. Wang, K. Xia, H. Wang, X. Liang, Z. Yin and Y. Zhang, *Adv. Mater.*, 2019, **31**, 1801072.
5. J. H. Koo, D. C. Kim, H. J. Shim, T.-H. Kim and D.-H. Kim, *Adv. Funct. Mater.*, 2018, **28**, 1801834.
6. S. B. Singh, T. Kshetri, T. I. Singh, N. H. Kim and J. H. Lee, *Chem. Eng. J.*, 2019, **359**, 197-207.
7. D. Toybou, C. Celle, C. Aude-Garcia, T. Rabilloud and J. P. Simonato, *Environ. Sci. Nano*, 2019, **6**, 684-694.
8. <https://www.electronics.ca/nanoelectronics-market-report.html>
9. <https://www.electronics.ca/store/markets-for-silver-nanomaterials-as-transparent-conductors.html>
10. <https://www.electronics.ca/store/nanomaterials-transparent-printable-electronics.html>